Gas-particle Flows Over a Wavy Wall

By

Ryuji Ishii

(Received August 13, 1984)

Summary

This paper describes a theoretical investigation into the perturbation problem of gas-particle two-phase flows over a wavy wall. It is assumed that the gas is inviscid except for its interaction with the particles, and no phase change takes place. The flow region is split into two sub-regions, an inner region near the wavy wall, where particle-free regions appear, and an outer region above the inner region. The inner and the outer expansions are matched with each other in some overlapping domain. The inner problem is solved numerically, and the outer problem is solved analytically. Main attention is paid to the flow structure near the wavy wall, and also the drag of the wavy wall.

Introduction

There are many engineering applications for flows of a medium that consists of a suspension of powdered material or liquid droplets in a gas. The system of governing equations for a dusty gas is very similar to that for vibrationally or chemically relaxing dust-free gases. The effects of vibrational and chemical relaxations on the gas flow are well understood, particularly in the linear regime (Vincenti 1959, Clarke 1959). There are, however, a few important differences between the relaxation phenomena in a dust-free gas with relaxing internal modes and those in a dusty gas. One of the most important differences is that the velocities of the particles can be, in general, different from the gas velocity, leading to distinct momentum equations for the gas and the particles that are coupled with each other. This is not the case for the relaxing dust-free gases. Especially for multi-dimensional two-phase flows, the particle streamlines can deviate from the gas streamlines, which usually introduces a great mathematical difficulty into their analysis (Ishii & Kawasaki 1982, Miura 1974). It is, therefore, impossible for us to apply previous solutions for relaxing dust-free gases directly to flows of gas-particle mixtures even in linearized problems.

Department of Aeronautics, Kyoto University, Kyoto 606, Japan

In this paper, a perturbation flow of gas-particle mixtures over a sinusoidal wall is considered. The problem is treated as a perturbation from a uniform reference flow. The flow region is divided into two sub-regions, the thin inner layer near the wall where the particle-free regions appear, and the outer region above the inner layer.

Essentially, as will be seen later, the system of equations for the perturbation quantities is not linear for the inner flow. This system will, however, be proved to be treated substantially as a linear one. The inner problem is analyzed numerically by the method of characteristics for a supersonic reference flow. The particle trajectories are investigated in detail to obtain the location of particle-free-regions.

The system of perturbation equations for the outer region is a linear one, and then the outer problem is solved analytically by means of the Laplace transform for a supersonic reference flow. Only for the limiting case of the infinitely wavy wall, the outer problem is solved directly by the previous method applied by Vincenti (1959).

The matching technique to be employed here relies on the hypothesis that the outer expansion fits the inner expansion in some overlapping domain.

Sample calculations are carried out for a mixture composed of air and small solid particles of Al_2O_3.

Assumptions

The gas-particle mixture is supposed to be in equilibrium in the reference state. The analysis will be based on the following assumptions:

(1) No phase change takes place.
(2) The viscous force acting on each particle obeys Stokes' law.
(3) The heat transfer rate to each particle is proportional to the temperature difference between the gas and the particle.
(4) The gas is inviscid except for its interaction with the particles.
(5) The gas is a perfect gas with constant composition and constant specific heats.
(6) The volume occupied by the particles is neglected.
(7) The thermal and Brownian motions of the particles are negligible.
(8) The particles do not interact with each other.
(9) The particles are solid spheres with a uniform diameter and a constant material density.

(10) The particles have a constant specific heat, and the internal temperature of the particles is uniform.

(11) The particles which impinge on the wall make a perfectly inelastic collision with the wall, and they adhere to or are absorbed by the wall after the impingement.

(12) The impinged particles on the wall do not change the shape of the wall.

Obviously, the assumption (12) is consistent with (6). These assumptions have been used in many previous papers treating gas-particle flows (Marble 1963, Rudinger 1975, Carrier 1958, Takano & Adachi 1975).

Basic Equations

We begin by setting down the equations of gas dynamics for a steady two-dimensional flow of the gas-particle mixture. Within the assumptions given in the previous chapter, the governing equations are given in the xy coordinate system as follows (Zucrow & Hoffman 1977):

$$\nabla(\rho \boldsymbol{V}) = 0, \tag{1}$$

$$\rho \frac{D}{Dt}\boldsymbol{V} + \nabla P = -\rho_p A_p(\boldsymbol{V} - \boldsymbol{V}_p), \tag{2}$$

$$\rho \frac{D}{Dt}\left(\frac{\gamma}{\gamma-1}\frac{P}{\rho} + \frac{1}{2}\boldsymbol{V}^2\right) = -\rho_p\{B_p(T-T_p) + A_p \boldsymbol{V}_p(\boldsymbol{V}-\boldsymbol{V}_p)\}, \tag{3}$$

$$P = R\rho T, \tag{4}$$

$$\nabla(\rho_p \boldsymbol{V}_p) = 0, \tag{5}$$

$$\frac{D_p}{Dt}\boldsymbol{V}_p = A_p(\boldsymbol{V}-\boldsymbol{V}_p), \tag{6}$$

$$\frac{D_p}{Dt}T_p = \frac{B_p}{C_{pp}}(T-T_p), \tag{7}$$

where

$$\nabla = \boldsymbol{i}\frac{\partial}{\partial x} + \boldsymbol{j}\frac{\partial}{\partial y}, \tag{8}$$

$$\frac{D}{Dt} = \boldsymbol{V}\nabla, \tag{9}$$

$$\frac{D_p}{Dt} = \boldsymbol{V}_p\nabla. \tag{10}$$

In these equations, ρ, $\boldsymbol{V}$, P, and T are the density, the velocity, the pressure and the temperature of the gas. The subscript p denotes the quantities associated with the particles. The vectors $\boldsymbol{i}$ and $\boldsymbol{j}$ are the unit ones in the x and y directions,

respectively. The constants R and γ are the individual gas constant and the ratio of the specific heats for the gas phase, and C_{pp} is the specific heat of the particle material. The quantities A_p and B_p are the inverse relaxation times for the particle velocity and temperature, respectively, and are given under the assumptions (2) and (3) as

$$A_p = \frac{18\mu}{\rho_{mp} D_p^2}, \tag{11}$$

$$B_p = \frac{12\mu C_{pg}}{\rho_{mp} D_p^2 P_r}, \tag{12}$$

where μ, C_{pg}, P_r, ρ_{mp}, and D_p are the coefficient of viscosity, the specific heat at the constant pressure, the Prandtl number of the gas, the material density and the diameter of the particles. In the present case, the quantities A_p and B_p are related with each other by

$$B_p = \frac{2C_{pg}}{3P_r} A_p . \tag{13}$$

Wall geometry

Consider a semi-infinitely sinusoidal wall described by

$$y_w = \begin{cases} 0 & \text{for } x<0, \\ y_0 \sin\left(2\pi \dfrac{x}{l}\right) & \text{for } x>0, \end{cases} \tag{14}$$

as shown in Fig. 1, where l is the wave length, y_0 is the amplitude and the subscript w denotes the wall boundary. Now, for later convenience, the non-dimensionalized coordinates of x and y are introduced by

$$x' = x \Big/ \left(\frac{l}{2\pi}\right), \quad y' = y \Big/ \left(\frac{l}{2\pi}\right). \tag{15}$$

With these, Equation (14) is rewritten as

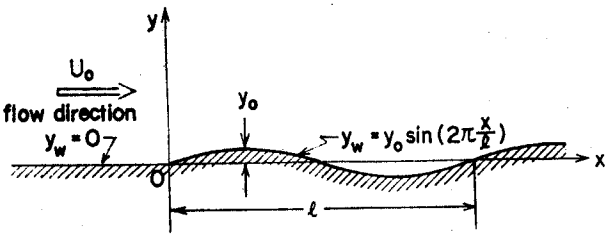

Fig. 1. Sinusoidally wavy wall.

$$y'_w = \begin{cases} 0 & \text{for } x'<0\,, \\ \varepsilon \sin x' & \text{for } x'>0\,, \end{cases} \tag{16}$$

where

$$\varepsilon = y_0 \Big/ \left(\frac{l}{2\pi}\right). \tag{17}$$

Since our ultimate concern is with the small-disturbance flow over the wavy wall, we shall assume that

$$\varepsilon \ll 1\,. \tag{18}$$

In the present analysis, under the condition (18), we assume that the flowfield can be described by a perturbation on a uniform parallel flow with velocity U_0 in the x direction. Although it is assumed that the reference flow is supersonic, it will be proved that some part of the present result remains valid for the subsonic reference flow.

Perturbation Equations

The perturbation quantities are now introduced by

$$\begin{aligned} \boldsymbol{V} &= U_0(\boldsymbol{i}+\varepsilon \boldsymbol{q}+O(\varepsilon^2))\,, \\ P &= P_0(1+\varepsilon p+O(\varepsilon^2))\,, \\ \rho &= \rho_0(1+\varepsilon \sigma+O(\varepsilon^2))\,, \\ T &= T_0(1+\varepsilon \tau+O(\varepsilon^2))\,, \\ \boldsymbol{V}_p &= U_0(\boldsymbol{i}+\varepsilon \boldsymbol{q}_p+O(\varepsilon^2))\,, \\ \rho_p &= \rho_{p0}(1+\varepsilon \sigma_p+O(\varepsilon^2))\,, \\ T_p &= T_0(1+\varepsilon \tau_p+O(\varepsilon^2)) \end{aligned} \tag{19}$$

where

$$\boldsymbol{q} = u\boldsymbol{i}+v\boldsymbol{j}\,, \tag{20}$$

and subscript zero denotes the unperturbed reference state.

Before deriving the perturbation equations from Equations (1) to (7) with (15), (19), and (20), attention must be paid to the flow field near the wavy wall. In Figure 2, the gas and the particle streamlines near the wall are shown schematically under the conditions (11) and (12), where the shaded regions are the dust-free regions and the solid and dotted lines are the gas and particle streamlines. Appearance of such dust-free regions usually introduces a great mathematical difficulty. Since it will be reasonable to consider that the extent of such dust-free regions in the $x'y'$ plane may be controlled mainly by the geometric parameter ε, the flow region

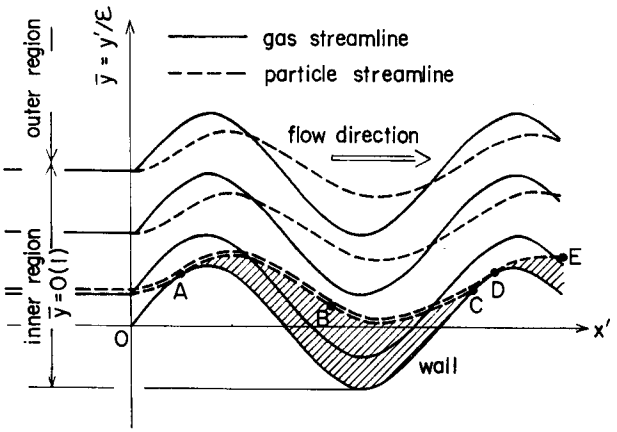

Fig. 2. Flowfield near the wavy wall.

is divided into two sub-regions, the inner and the outer regions, as shown in Figure 2. The perturbation equations are then derived separately for each region.

A. The inner expansion

In order to solve the inner problem, it is convenient to introduce a new coordinate system $(x', \bar{y})$, where $\bar{y}$ is given by

$$\bar{y} = y'/\epsilon \,. \tag{21}$$

Substituting Equation (19) into Equations (1) to (7) in conjunction with (8), (20), and (21), we have for the fitsr-order perturbation quantities:

$$\frac{\partial v}{\partial \bar{y}} = 0, \tag{22}$$

$$\left(\frac{\partial}{\partial x'} + v\frac{\partial}{\partial \bar{y}}\right)u + \frac{1}{\gamma M^2}\frac{\partial p}{\partial x'} = -\alpha\nu E(u-u_p)\,, \tag{23}$$

$$\frac{\partial p}{\partial \bar{y}} = 0\,, \tag{24}$$

$$\left(\frac{\partial}{\partial x'} + v\frac{\partial}{\partial \bar{y}}\right)\{\tau + (\gamma-1)M^2u\} = -\beta\nu\theta E(\tau-\tau_p) - (\gamma-1)\alpha\nu EM^2(u-u_p)\,, \tag{25}$$

$$p = \sigma + \tau\,, \tag{26}$$

$$\frac{\partial v_p}{\partial \bar{y}} = 0, \tag{27}$$

$$\left(\frac{\partial}{\partial x'} + v_p\frac{\partial}{\partial \bar{y}}\right)u_p = \alpha(u-u_p)\,, \tag{28}$$

$$\frac{\partial v_p}{\partial x'} = \alpha(v - v_p), \tag{29}$$

$$\left(\frac{\partial}{\partial x'} + v_p \frac{\partial}{\partial y}\right)\tau_p = \beta(\tau - \tau_p), \tag{30}$$

where

$$\alpha = \frac{A_{p0} l}{2\pi U_0} \tag{31}$$

$$\beta = \frac{B_{p0} l}{2\pi U_0 C_{pp}} \tag{32}$$

$$M = U_0 \Big/ \sqrt{\gamma \frac{P_0}{\rho_0}} \tag{33}$$

$$\theta = C_{pp}/C_{pg}, \tag{34}$$

$$\nu = \rho_{p0}/\rho_0. \tag{35}$$

The quantity M is the Mach number of the reference flow associated with the speed of sound for the gas phase, and ν is the loading ratio.

This system is not linear because Equations (23), (25), (28), and (30) involve terms with $v\partial/\partial y$ and $v_p\partial/\partial y$. Fortunately, however, it will be shown later that this system can be treated substantially as a linear one. As is demonstrated in Figure 2, there are particle free regions in the inner layer. This situation is taken into account by introducing the quantity E in Equations (23) and (25). This is defined as

$$E = \begin{cases} 1 & \text{for a dusty region,} \\ 0 & \text{for a dust-free region,} \end{cases} \tag{36}$$

which means that the quantity E can be taken as a function of the particle streamline.

Here, it must be pointed out that there is no equation involving the perturbation quantity σ_p. This suggests that the particle density σ_p cannot be determined in the first-order perturbation problem in the present analysis. (See Appendix A.) Equations (22) to (30) then constitute a system of nine equations for eight unknowns u, v, p, τ, σ, u_p, v_p, and τ_p. Mathematically, this system is considered to be an over-determined system.

The boundary conditions imposed on this system are

$$v = \begin{cases} 0 & \text{for } x' < 0, \\ \cos x' & \text{for } x' > 0, \end{cases} \tag{37}$$

at $y = y_w = \sin x'$, and that the inner solution must fit the outer solution in the vicinity of $y = \infty$.

B. The outer expansion

In the outer region, Equations (1) to (7) are linearized in the $x'y'$ coordinate system just as in the previous analyses for relaxing dust-free gases. Substituting Equation (19) into Equations (1) to (7) in conjunction with Equations (8) and (20), we have

$$\frac{\partial \sigma}{\partial x'}+\nabla' \boldsymbol{q}=0\,, \tag{38}$$

$$\frac{\partial \boldsymbol{q}}{\partial x'}+\frac{1}{\gamma M^2}\nabla' p=-\alpha\nu(\boldsymbol{q}-\boldsymbol{q}_p) \tag{39}$$

$$\frac{\partial}{\partial x'}\{p-\sigma+(\gamma-1)M^2u\}=-\beta\nu\theta(\tau-\tau_p)-(\gamma-1)\alpha\nu M^2(u-u_p)\,, \tag{40}$$

$$p=\sigma+\tau\,, \tag{41}$$

$$\frac{\partial \sigma_p}{\partial x'}+\nabla' \boldsymbol{q}_p=0\,, \tag{42}$$

$$\frac{\partial \boldsymbol{q}_p}{\partial x'}=\alpha(\boldsymbol{q}-\boldsymbol{q}_p)\,, \tag{43}$$

$$\frac{\partial \tau_p}{\partial x'}=\beta(\tau-\tau_p)\,, \tag{44}$$

where

$$\nabla'=\boldsymbol{i}\frac{\partial}{\partial x'}+\boldsymbol{j}\frac{\partial}{\partial y'}\,. \tag{45}$$

This system constitutes a set of nine equations for nine variables, and is solved for the boundary conditions

$$\{\sigma,\ \boldsymbol{q},\ p,\ \tau,\ \sigma_p,\ \boldsymbol{q}_p,\ \tau_p\}=\text{finite as } y'\to\infty, \tag{46}$$

and also that the outer solution must fit the inner one in the vicinity of $y'\to 0$.

Solutions of the Perturbation Equations

As has been discssued previously, the inner and the outer problems are coupled with each other by the boundary conditions. These problems, therefore, must be solved simultaneously. In the present analysis, first the inner problem is partly solved. Then, the outer solution is obtained by making use of the matching principle. Finally, the remaining part of the inner problem is solved numerically.

The inner solution

In the inner problem, it is impossible to shift the boundary surface (16) to the basic position of the wavy wall, $y=0$, as in the usual linearized problems of

dust-free gases. The reason is that in the $x'\bar{y}$ plane, the amplitude of the wavy wall is order unity.

From Equations (22), (24), and (27), we can get

$$v = \phi(x') , \tag{47}$$

$$v_p = \phi_p(x') , \tag{48}$$

$$p = \psi(x') , \tag{49}$$

respectively, showing that these variables are the functions of x' only, and do not depend on $\bar{y}$. By considering the boundary condition (37), it is given that

$$\phi(x') = \begin{cases} 0 & \text{for } x'<0 , \\ \cos x' & \text{for } x'>0 , \end{cases} \tag{50}$$

with which Equation (29) is solved to yield

$$\phi_p(x') = \begin{cases} 0 & \text{for } x'<0 , \\ \dfrac{\alpha}{\alpha^2+1}\{\alpha\cos x'+\sin x'-\alpha\exp(-\alpha x')\} & \text{for } x'>0 . \end{cases} \tag{51}$$

These results indicate an important fact that the perturbation velocities v and v_p in the inner layer do not depend on the loading ratio ν. In particular, the gas velocity $\phi(x')$ is completely independent of the existing particles. As will be seen later, the pressure distribution $\psi(x')$ can be determined by the matching procedure with the outer expansion.

With Equations (47) to (49), the system of equations is rearranged in the following form:

$$\left(\frac{\partial}{\partial x'}+\phi(x')\frac{\partial}{\partial \bar{y}}\right)u+\frac{1}{\gamma M^2}\frac{d\psi(x')}{dx'} = -\alpha\nu E(u-u_p) , \tag{52}$$

$$\left(\frac{\partial}{\partial x'}+\phi(x')\frac{\partial}{\partial \bar{y}}\right)\{\tau+(\gamma-1)M^2u\}$$

$$= -\beta\nu\theta E(\tau-\tau_p)-(\gamma-1)\alpha\nu EM^2(u-u_p), \tag{53}$$

$$\sigma+\tau = \psi(x') , \tag{54}$$

$$\left(\frac{\partial}{\partial x'}+\phi_p(x')\frac{\partial}{\partial \bar{y}}\right)u_p = \alpha(u-u_p) , \tag{55}$$

$$\left(\frac{\partial}{\partial x'}+\phi_p(x')\frac{\partial}{\partial \bar{y}}\right)\tau_p = \beta(\tau-\tau_p) . \tag{56}$$

These now constitute a system of five equations for five unknowns: u, τ, σ, u_p, and τ_p, and they obviously are linear for these unknowns. This system can be solved once the pressure $\psi(x')$ is known.

Before discussing the method for solving the problem, the gas and the particle trajectories in the inner layer are obtained. These are not only necessary in order to solve the system but also very interesting theoretically. In the present first-order perturbation, the gas and the particle trajectories are given, respectively, by

$$\bar{\eta} = \text{const} \quad \text{along} \quad \frac{d\bar{y}}{dx'} = v\,, \tag{57}$$

$$\bar{\eta}_p = \text{const} \quad \text{along} \quad \frac{d\bar{y}}{dx'} = v_p\,, \tag{58}$$

where $\bar{\eta}=\eta/\varepsilon$ and $\bar{\eta}_p=\eta_p/\varepsilon$. These quantities are the functions of x' and $\bar{y}$, which are obtained by solving

$$\frac{\partial\bar{\eta}}{\partial x'}\Big/\frac{\partial\bar{\eta}}{\partial\bar{y}} = -v\,, \tag{59}$$

$$\frac{\partial\bar{\eta}_p}{\partial x'}\Big/\frac{\partial\bar{\eta}_p}{\partial\bar{y}} = -v_p\,. \tag{60}$$

It will be easy to realize that Equations (59) and (60) were derived from Equations (57) and (58), respectively. For the explicit determination of $\bar{\eta}(x', \bar{y})$ and $\bar{\eta}_p(x', y)$, a so-called labeling of these variables is necessary, because the relations between $(\bar{\eta}, \bar{\eta}_p)$ and $(x', \bar{y})$ have been given by the first-order differential Equations (59) and (60). Mathematically, the labeling of these streamline variables is equivalent to the specification of the arbitrary integral functions in the general solutions for Equations (59) and (60). Here, the gas (particle) streamline which traverses the $\bar{y}$ axis $(x'=0)$ at $\bar{y}=\bar{y}_1$ $(\bar{y}=\bar{y}_2)$ is labeled as $\bar{\eta}=\bar{y}_1$ $(\bar{\eta}_p=\bar{y}_2)$. For such labelings, Equations (59) and (60) are solved in conjunction with (47), (48), (50), and (51) to yield, respectively,

$$\bar{\eta} = \begin{cases} \bar{y} & \text{for } x'<0\,, \\ \bar{y}-\sin x' & \text{for } x'>0\,, \end{cases} \tag{61}$$

$$\bar{\eta}_p = \begin{cases} \bar{y} & \text{for } x'<0\,, \\ \bar{y}-\dfrac{\alpha}{\alpha^2+1}\{\alpha\sin x'-\cos x'+\exp(-\alpha x')\} & \text{for } x'>0\,. \end{cases} \tag{62}$$

It will be easy to see that the gas streamline along the wall is denoted by $\bar{\eta}=0$. As for the particle streamline, the situation is very complicated, since the impingement of the particles on the wavy wall may occur for $x'>0$. In Figure 2, the wall portions OA and CD are the regions where the particles impinge. The particle streamlines ABC and DE, which divide the dusty and dust-free regions,

are the so-called limiting particle streamlines. It must be noticed that the limiting particle streamlines $\overline{\eta}_{pABC}$ and $\overline{\eta}_{pDE}$ are different. Such a situation is, of course, based on the assumptions (11) and (12).

Previous discussion suggested that the occurrence of absorption cf the impinged particles by the wall must be taken into account in the description of the particle streamline near the wavy wall by Equation (62). Considering the fact that the wavy wall is described by $\bar{y}=\sin x'$ ($\overline{\eta}=0$), we can represent the particle streamlines on the wavy wall by

$$\overline{\eta}_{pw}(x') = \begin{cases} 0 & \text{for } x'<0, \\ \sin x' - \dfrac{\alpha}{\alpha^2+1}\{\alpha \sin x' - \cos x' + \exp(-\alpha x')\} & \text{for } x'>0, \end{cases} \tag{63}$$

$$\overline{\eta}_{pw}(x_2') \geqq \overline{\eta}_{pw}(x_1') \qquad \text{for } x_2'>x_1', \tag{64}$$

where the second equation represents the effect of absorption of impinged particles by the wall. Figure 3 shows $\overline{\eta}_{pw}$ for $\alpha=1.0$, where there exist some ranges of x', for which $\overline{\eta}_{pw}$ satisfying the Equations (63) and (64) cannot be found. In such regions, there appear particle-free regions surrounded by limiting particle streamlines and the wall boundary. For a few values of α, the limiting particle streamlines are shown in Figures 3, 4, and 5. Figure 6 demonstrates the limiting particle streamlines in the physical plane for $\alpha=1.0$.

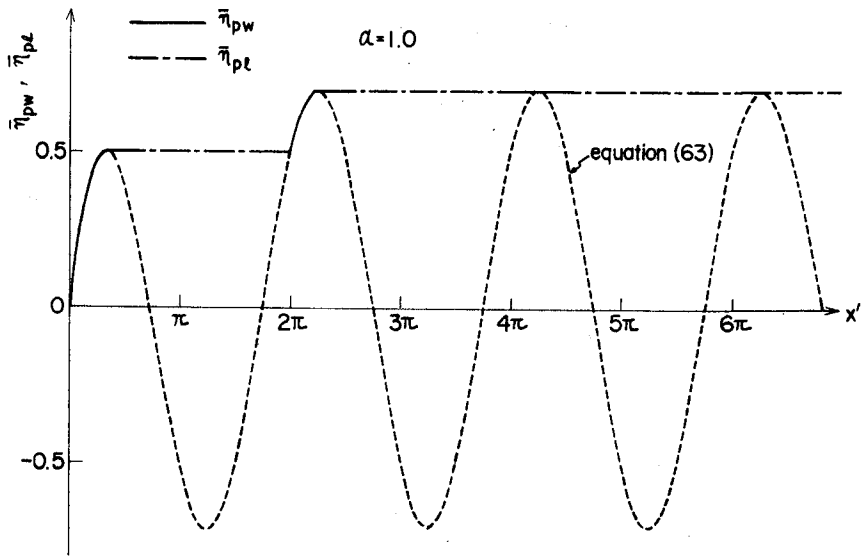

Fig. 3. Particle streamline on the wavy wall.

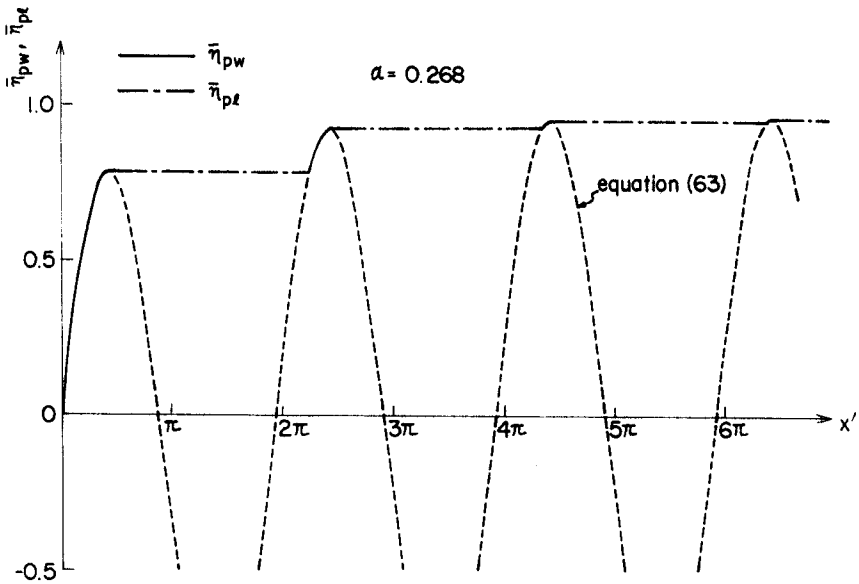

Fig. 4. Particle streamline on the wavy wall.

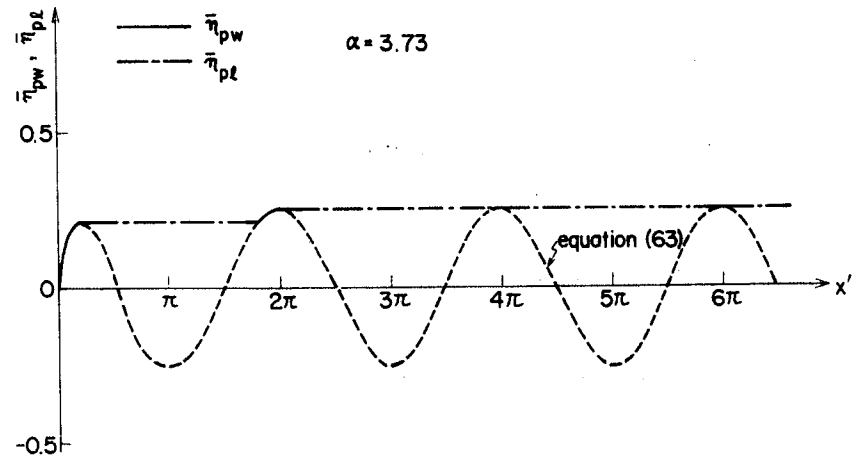

Fig. 5. Particle streamline on the wavy wall.

Since the flow structure becomes completely periodic as $x' \to \infty$, the impingement of particles on the wavy wall will cease in the limit $x' \to \infty$. This means that the limiting particle streamline $\bar{\eta}_{pl}$ converges to some value $\bar{\eta}_{pl\infty}$ as $x' \to \infty$, where the subscript l denotes the limiting particle streamline. Furthermore, it can be concluded that this value $\bar{\eta}_{pl\infty}$ gives the total amount of impinged particles on the wavy wall in the range $0 < x' < \infty$, since $\bar{\eta}_{pw}(0) = 0$. With Equations (63) and (64), $\bar{\eta}_{pl\infty}$ can be obtained as

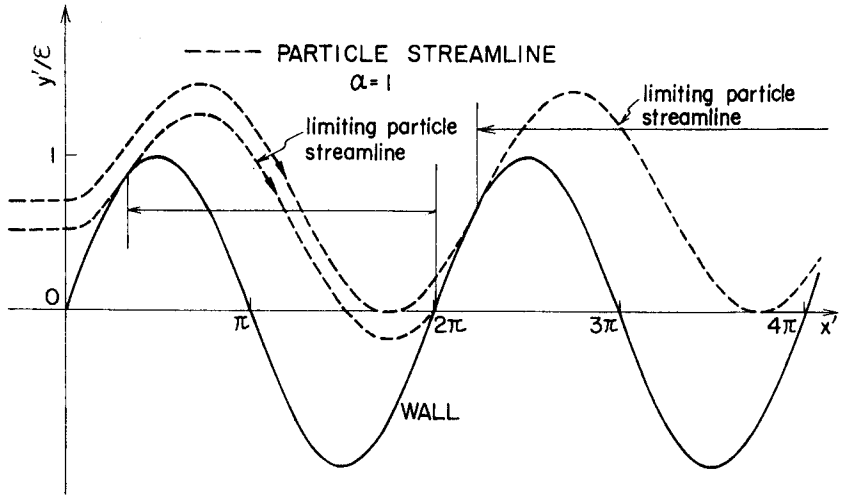

Fig. 6. Limiting particle streamline in the $x'\bar{y}$ plane.

$$\bar{\eta}_{pl\infty} = 1/\sqrt{\alpha^2+1}. \tag{65}$$

By making use of this result, the location of the limiting particle streamline can be given from Equation (62) as

$$\bar{y} = \frac{\alpha}{\alpha^2+1}(\alpha \sin x' - \cos x') + \frac{1}{\sqrt{\alpha^2+1}}, \tag{66}$$

for $x' \gg 1$.

As has been discussed previously, the particle-free regions are surrounded by the limiting particle streamlines and the wall boundary. Then, these regions are mathematically defined by

$$\bar{\eta}_p(x', \bar{y}) < \bar{\eta}_{pl}(x'), \tag{67}$$

$$\bar{\eta}(x', \bar{y}) > 0. \tag{68}$$

For an infinitely large x', Equation (67) can be rewritten as

$$\bar{\eta}_p(x', \bar{y}) < \bar{\eta}_{pl\infty} = \text{const.} \tag{69}$$

Since $\bar{\eta}_p(x', \bar{y})$ (in Equation (62)) and then $\bar{\eta}_{pl}(x')$ involve only one parameter α, the location or the extent of the particle-free regions in the $x'\bar{y}$ plane depends on this parameter α only. In other words, the particle-free regions in the $x'y'$ plane are controlled by only two parameters, the wall parameter ϵ and the particle parameter α.

Now, we return to the problem of solving the system of Equations (52) to

(56). With Equations (61) and (62), these equations are easily rewritten in the form,

$$\frac{du}{dx'}+\frac{1}{\gamma M^2}\frac{d\psi}{dx'} = -\alpha\nu E(\bar{\eta}_p)(u-u_p)\,, \tag{70}$$

$$\frac{d}{dx'}\{\tau+(\gamma-1)M^2u\} = -\beta\nu\theta E(\bar{\eta}_p)(\tau-\tau_p)-(\gamma-1)\alpha\nu E(\bar{\eta}_p)M^2(u-u_p)\,, \tag{71}$$

along $\bar{\eta}$ = const,

where

$$E(\bar{\eta}_p) = \begin{cases} 0 & \text{for } \bar{\eta}_p<\bar{\eta}_{pl} \text{ (dust-free region)}\,, \\ 1 & \text{for } \bar{\eta}_p\geqq\bar{\eta}_{pl} \text{ (dusty region)}\,, \end{cases} \tag{72}$$

$$\sigma = \psi-\tau\,, \tag{73}$$

and

$$\frac{du_p}{dx'} = \alpha(u-u_p)\,, \tag{74}$$

$$\frac{d\tau_p}{dx'} = \beta(\tau-\tau_p)\,, \tag{75}$$

along $\bar{\eta}_p$ = const.

Obviously, these are given in the characteristic form, and then easily solved numerically, once $\psi(x')$ is given.

The boundary conditions imposed on the system are

$$u = -1/\sqrt{M^2-1}, \tag{76}$$

$$\tau = (\gamma-1)M^2/\sqrt{M^2-1}, \tag{77}$$

$$u_p = 0\,, \tag{78}$$

$$\tau_p = 0\,. \tag{79}$$

at $x'=0$ (See Appendix B.)

The outer solution

Although the inner problem has been solved only partly, the outer problem can now be solved by using the partial inner solution. Making use of the matching principle, we can get the boundary conditions for the outer problem from the results in the previous section as follows,

$$v \to \phi(x') \qquad \text{as } y' \to 0\,, \tag{80}$$

$$v_p \to \phi_p(x') \qquad \text{as } y' \to 0 \tag{81}$$

in addition to Equation (46). The condition (81) substantially means that there is no need to consider the phenomenon of particle impingement on the wall and

therefore there is no need to introduce the function E as in Equation (72) in the outer problem.

Combining Equations (39) and (43), we have

$$\frac{\partial}{\partial x'}\left\{\frac{\partial}{\partial x'}+\alpha(\nu+1)\right\}\left(\frac{\partial v}{\partial x'}-\frac{\partial u}{\partial y'}\right)=0\,.$$

Since the reference flow is uniform and irrotational, this is integrated to yield

$$\frac{\partial v}{\partial x'}-\frac{\partial u}{\partial y'}=0 \tag{82}$$

which means that the flow in the outer region is also irrotational. In a similar manner, the x' component of Equation (39) and Equation (40) are integrated to yield

$$p+\gamma M^2(u+\nu u_p)=0\,, \tag{83}$$

$$\tau+\nu\theta\tau_p+(\gamma-1)M^2(u+\nu u_p)=0\,, \tag{84}$$

respectively. Eliminating u, p, τ, σ, u_p, v_p and τ_p from Equations (38), (41), (43), (44), and (82) to (84), we have the following equation for v:

$$\frac{\partial^2}{\partial x'^2}\left(\Gamma_0\frac{\partial^2 v}{\partial x'^2}-\frac{\partial^2 v}{\partial y'^2}\right)+(a+b)\frac{\partial}{\partial x'}\left(\Gamma_1\frac{\partial^2 v}{\partial x'^2}-\frac{\partial^2 v}{\partial y'^2}\right)+ab\left(\Gamma_2\frac{\partial^2 v}{\partial \lambda'^2}-\frac{\partial^2 v}{\partial y'^2}\right)=0, \tag{85}$$

where

$$\Gamma_0=M^2-1\,,$$

$$\Gamma_1=M^2\frac{\left\{a(1+\nu)+b\left(\dfrac{1+\gamma\nu\theta}{1+\nu\theta}\right)\right\}}{(a+b)}-1\,, \tag{86}$$

$$\Gamma_2=M^2\frac{(1+\nu)(1+\gamma\nu\theta)}{(1+\nu\theta)}-1\,,$$

$$a=\alpha\,,$$

$$b=\beta(1+\nu\theta)\,. \tag{87}$$

Parameters a and b are introduced on purpose to emphasize the symmetric dependence of Equation (85) on these parameters.

For the supersonic reference flow, all the disturbances are identically zero upstream from the wavy wall. We, therefore, define the Laplace transform of quantity f by

$$\hat{f}(s,y')=\int_0^\infty f(x',y')\exp(-sx')dx'\,, \tag{88}$$

where f is any disturbance variable. It follows that v satisfies the equation

$$\frac{d^2\hat{v}}{dy'^2} = \frac{s^2\{\Gamma_0 s^2+(a+b)\Gamma_1 s+ab\Gamma_2\}}{(s+a)(s+b)}\hat{v}\,. \tag{89}$$

By considering the boundary condition (80) in conjunction with (50), it is given that

$$\hat{v}(s,\,0) = \frac{s}{s^2+1}\,, \tag{90}$$

with which, and with Equation (46), Equation (89) yields a solution for $\hat{v}$ in the form

$$\hat{v} = \frac{s}{s^2+1}\exp\left\{-s\sqrt{\frac{\Gamma_0(s+\lambda_1)(s+\lambda_2)}{(s+a)(s+b)}}\,y'\right\}. \tag{91}$$

Here, $(-\lambda_1,\,-\lambda_2)$ is a set of solutions for

$$\Gamma_0 s^2+(a+b)\Gamma_1 s+ab\Gamma_2 = 0. \tag{92}$$

As is shown in APPENDIX C, these two quantities λ_1 and λ_2 are real. With Equation (91), Equations (82) and (43) are solved to yield

$$\hat{u} = -\frac{s}{s^2+1}\sqrt{\frac{(s+a)(s+b)}{\Gamma_0(s+\lambda_1)(s+\lambda_2)}}\exp\left\{-s\sqrt{\frac{\Gamma_0(s+\lambda_1)(s+\lambda_2)}{(s+a)(s+b)}}\,y'\right\}, \tag{93}$$

$$\hat{u}_p = -\frac{as}{(s+a)(s^2+1)}\sqrt{\frac{(s+a)(s+b)}{\Gamma_0(s+\lambda_1)(s+\lambda_2)}}\exp\left\{-s\sqrt{\frac{\Gamma_0(s+\lambda_1)(s+\lambda_2)}{(s+a)(s+b)}}\,y'\right\}, \tag{94}$$

$$\hat{v}_p = \frac{as}{(s+a)(s^2+1)}\exp\left\{-s\sqrt{\frac{\Gamma_0(s+\lambda_1)(s+\lambda_2)}{(s+a)(s+b)}}\,y'\right\}, \tag{95}$$

Also, from Equation (83), we have

$$\hat{p} = -\gamma M^2(\hat{u}+\nu\hat{u}_p)\,. \tag{96}$$

Although the transforms of other perturbations τ, σ, τ_p, and σ_p can easily be obtained, these are not recorded here.

Generally, the inverse of the transforms on the right hand side of Equations (91) and (93) to (95) is very difficult (Clarke 1969). However, since we are sometimes most concerned about the distributions of flow variables near the wall, these transforms are inverted only for $y'\to 0$.

In the limit of $y'\to 0$, the exponential factors in Equations (91) and (93) to (95) are replaced by unity. Following the results by Erdelyi et al. (1954), we have:

$$u = -\frac{1}{\sqrt{\Gamma_0}}\int_0^{x'} f_1(z)f_2(x'-z)dz + f_2(x') , \tag{97}$$

$$u_p = -\frac{a}{\sqrt{\Gamma_0}}\int_0^{x'} f_{p1}(z)f_{p2}(x'-z)dz , \tag{98}$$

(See APPENDIX D.)
where

$$\begin{aligned} f_1(x') &= \frac{(b-\lambda_2)}{2}\exp\left\{-\frac{1}{2}(b+\lambda_2)x'\right\}\left\{I_0\left(\frac{b-\lambda_2}{2}x'\right)+I_1\left(\frac{b-\lambda_2}{2}x'\right)\right\} , \\ f_2(x') &= I_0\left(\frac{\lambda_1-a}{2}x'\right)\exp\left\{-\frac{1}{2}(\lambda_1+a)x'\right\} \\ &\quad +\int_0^{x'}\{a\cos(x'-\zeta)-\sin(x'-\zeta)\}I_0\left(\frac{\lambda_1-a}{2}\zeta\right)\exp\left\{-\frac{1}{2}(\lambda_1+a)\zeta\right\}d\zeta , \end{aligned} \tag{99}$$

$$\begin{aligned} f_{p1}(x') &= \exp\left\{-\frac{1}{2}(a+b)\frac{\Gamma_1}{\Gamma_0}x'\right\}I_0\left(\frac{\lambda_2-\lambda_1}{2}x'\right) , \\ f_{p2}(x') &= I_0\left(\frac{a-b}{2}x'\right)\exp\left\{-\frac{1}{2}(a+b)x'\right\} \\ &\quad +\int_0^{x'}\{b\cos(x'-\zeta)-\sin(x'-\zeta)\}I_0\left(\frac{a-b}{2}\zeta\right)\exp\left\{-\frac{1}{2}(a+b)\zeta\right\}d\zeta , \end{aligned} \tag{100}$$

and z and ζ are dummy variables. In these equations, I_0 and I_1 are the zero- and the first-order modified Bessel functions of the first kind. It is obvious that the inverse transforms of v and v_p are equal to $\phi(x')$ and $\phi_p(x')$ in Equations (76) and (77), respectively. With the results (99) and (100), Equation (96) yields the pressure,

$$p = \frac{\gamma M^2}{\sqrt{\Gamma_0}}\left\{\int_0^{x'} f_1(z)f_2(x'-z)dz + f_2(x') + \nu a\int_0^{x'} f_{p1}(z)f_{p2}(x'-z)dz\right\} , \tag{101}$$

which is equal to $\psi(x')$ in Equation (49).

So far, we have been exclusively concerned with the outer solution in the limit of $y'\to 0$. For an arbitrary value of y', it is very difficult to obtain the inverse transforms on the right hand side of Equations (91) and (93) to (95). Fortunately, however, for a sufficiently large value of x', the structure of the flow-field becomes periodic, and then the Equation (85) can easily be solved directly. Here, an analytical solution for the outer problem for an arbitrary value of y' will be obtained only for a sufficiently large value of x' without making use of the method of the Laplace transform.

Assuming the solution of Equation (85) for $x'\gg 1$ in the form

$$v = F(y')\exp(ix') , \tag{102}$$

where $F(y')$ is the function of y' only to be determined, and i is the imaginary unit, we have from Equation (85)

$$\frac{d^2F}{dy'^2} = (Q_r+iQ_i)F\,, \tag{103}$$

where

$$\begin{aligned} Q_r &= -\frac{1}{(a^2+1)(b^2+1)}\{a^2b^2\Gamma_2+(a^2+b^2)\Gamma_1+ab(2\Gamma_1-\Gamma_0-\Gamma_2)+\Gamma_0\}\,, \\ Q_i &= \frac{(a+b)}{(a^2+1)(b^2+1)}\{(\Gamma_1-\Gamma_0)+ab(\Gamma_2-\Gamma_1)\}\,. \end{aligned} \tag{104}$$

From the relation

$$\Gamma_2>\Gamma_1>\Gamma_0\,,$$

it can be proved that

$$Q_i>0\,. \tag{105}$$

This condition suggests that the general solution for Equation (85) has the form (Vincenti 1959),

$$F = C_-\exp\{(\Delta+i\Lambda)y'\}+C_+\exp\{-(\Delta+i\Lambda)y'\}, \tag{106}$$

where Δ and Λ are positive constants defined by

$$(\Delta,\ \Lambda) = \left(\sqrt{\frac{1}{2}(Q_r+\sqrt{Q_r^2+Q_i^2})},\ \sqrt{\frac{1}{2}(-Q_r+\sqrt{Q_r^2+Q_i^2})}\right), \tag{107}$$

and C_+ and C_- are complex constants. With Equation (106), Equation (102) is rewritten as

$$v = C_-\exp\{\Delta y'+i(x'+\Lambda y')\}+C_+\exp\{-\Delta y'+i(x'-\Lambda y')\}\,. \tag{108}$$

If the complex conjugate of v is denoted by v^*, this conjugate v^* is also the solution of Equation (85), which leads to the result that the solution for Equation (85) can be constructed by a linear combination of v and v^*. Considering the boundary conditions (46) and (80) in conjunction with (50), we can get the final solution for v in the form,

$$v = \cos(x'-\Lambda y')\exp(-\Delta y')\,. \tag{109}$$

Substituting this into Equation (82) yields

$$u = \frac{1}{\sqrt{\Delta^2+\Lambda^2}}\sin(x'-\Lambda y'-\delta)\exp(-\Delta y')\,, \tag{110}$$

where

$$\tan\delta = \frac{\Lambda}{\Delta}\,. \tag{111}$$

Similarly, substituting Equations (109) and (110) into Equation (43) yields

$$u_p = -\frac{\alpha}{\sqrt{\alpha^2+1}}\frac{1}{\sqrt{\Delta^2+\Lambda^2}}\cos(x'-\Lambda y'-\delta+\delta_p)\exp(-\Delta y')\,, \tag{112}$$

$$v_p = \frac{\alpha}{\sqrt{\alpha^2+1}}\sin(x'-\Lambda y'+\delta_p)\exp(-\Delta y')\,, \tag{113}$$

where

$$\tan\delta_p = \alpha\,. \tag{114}$$

Now, the pressure p can be determined from (83) with Equations (110) and (112). The result is

$$p = -\frac{\gamma M^2}{\sqrt{\Delta^2+\Lambda^2}}\left\{\sin(x'-\Lambda y'-\delta)-\frac{\nu\alpha}{\sqrt{\alpha^2+1}}\cos(x'-\Lambda y'-\delta+\delta_p)\right\} \cdot\exp(-\Delta y')\,. \tag{115}$$

One important general result is stated. In the derivation of the results (109) to (115) and also the results (50) and (51), the condition that the reference flow should be supersonic has been essentially unnecessary. This means that the solutions (109) to (115) and also the results for the gas and the particle streamlines in the inner layer remain valid even for the subsonic reference flow. The detailed structure of the solutions (109) to (115) is nearly the same as that in the previous analyses of the linearized dust-free gas flows with the vibrational or the chemical relaxation over the wavy wall (Vincenti 1969).

Sample Calculations

By using the results obtained previously, sample calculations were carried out on the electronic digital computer FACOM 230 in the Computer Center of Kyoto University. A dusty gas composed of air and small solid particles of Al_2O_3 was considered. The physical constants and the reference conditions are listed in Table 1. The calculations were carried out only for the flow regions near the wavy wall. Unfortunately, however, the numerical results, except for v, v_p, and p, could not be obtained for $x' \gg 1$ in the inner problem, since some purely numerical difficulty appears for the downstream region of $x' \gg 1$. The details of this difficulty will be discussed later.

In spite of such a situation, it must be emphasized that the analytical inner

Table 1.

Physical constants

Air	Al_2O_3
$\gamma=1.4$ $C_{pg}=1005.0$ J/kgK $\mu=1.79\times10^{-5}$ kg/m sec (for $T_0=288.0$ K) $P_r=0.75$	$\rho_p=4.0\times10^3$ kg/m^3 $C_{pp}=1686.0$ J/kg K
Reference conditions	
$T_0=288.0$ K $\rho_0=1.23$ kg/m^3 $a_{f0}=340.0$ m/sec	

solutions for $v(\phi(x'))$ and $v_p(\phi_p/(x'))$ and the inner limits of the outer solutions for u, u_p, and $p(\psi(x'))$ are valid for all x', and their numerical results have been obtained for all x'. These results are sometimes sufficient for practical purposes, since the gas and the particle streamlines near the wavy wall and the pressure distribution on the wall are completely determined from these results.

In Figure 7, the distributions of the gas and the particle velocities, u and u_p, and the pressure p calculated from Equations (97), (98), and (101), respectively, are shown for $\nu=0.3$ and $\alpha=1.0$. These u, u_p, and p are the inner limits of the outer solutions, and especially this p is equal to $\psi(x')$. This figure indicates that these solutions become almost completely periodic after only a few times of

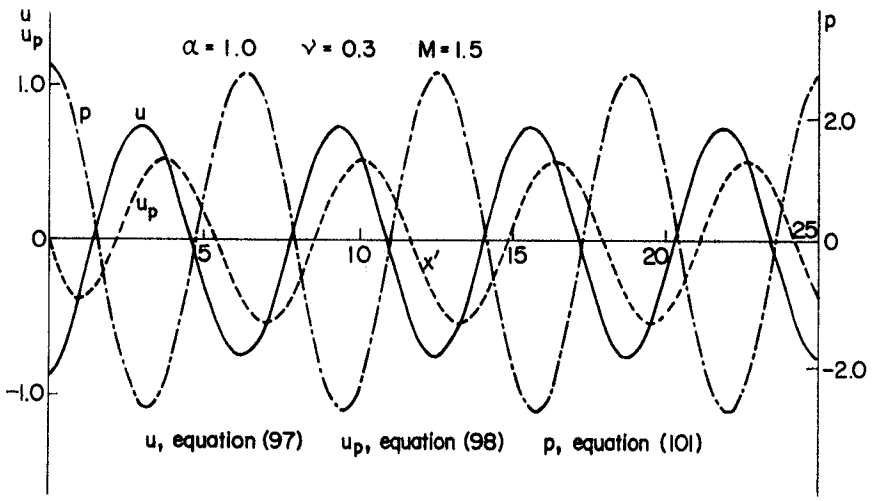

Fig. 7. Distributions of inner limits of outer solutions u, u_p, and p along x'.

the wavelength from the origin. It is easy to explain this situation with Equations (51), (97), and (98) in conjunction with Equations (99) and (100). As is proved in APPENDIX C, λ_1 and λ_2 are both positive, and the parameters a and b defined in Equation (87) are considered to be of the same order. Then, all the exponential terms in Equations (51), (97), and (98) are $O(\exp(-\alpha x'))$, which leads to the result that it takes only a short distance, $x'=O(1/\alpha)$, for these solutions to become almost periodic.

After determining the function $E(\bar{\eta}_b)$ with Equations (63) and (64), the system of Equations (70) to (75) was solved numerically by the method of characteristics, where Equation (101) was used as $\psi(x')$. Since the characteristics, which are the gas and the particle streamlines in the present case, are already known by Equations (61) and (62), the numerical procedure is very simple and easy. The accuracy of all the numerical results has been checked by comparing the results for a few different mesh sizes. The result for u along the gas streamline on the wavy wall ($\bar{\eta}=0$) is shown in Figure 8, being compared with the inner limit of the outer u (Equation (97)). The mesh sizes used in the present calculation are $\Delta x'=\pi/60$ and $\Delta\bar{\eta}=\pi/30$. The limiting particle streamlines corresponding to the results in Figures 7 and 8 are shown in Figure 9. It is interesting to note that Figure 8 suggests the existence of a velocity gradient in the $\bar{\eta}$ direction, which may be very large in magnitude because $\partial u/\partial\bar{\eta}$ is rewritten as $\varepsilon^{-1}(\partial u/\partial\eta)$ with the unstretched variable η. In order to investigate this situation in detail, the distributions of u along the $\bar{\eta}$ direction at several points x' are shown in Figures 10 to 16. These points x' are

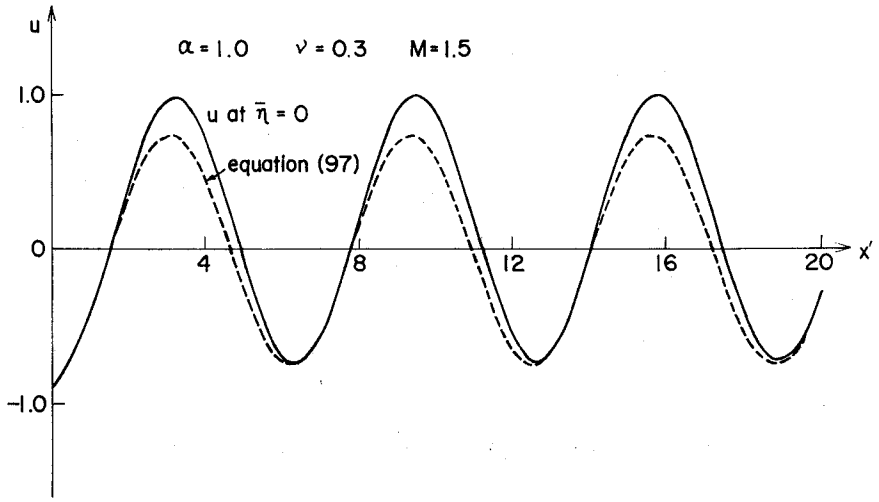

Fig. 8. Distribution of u along x'.

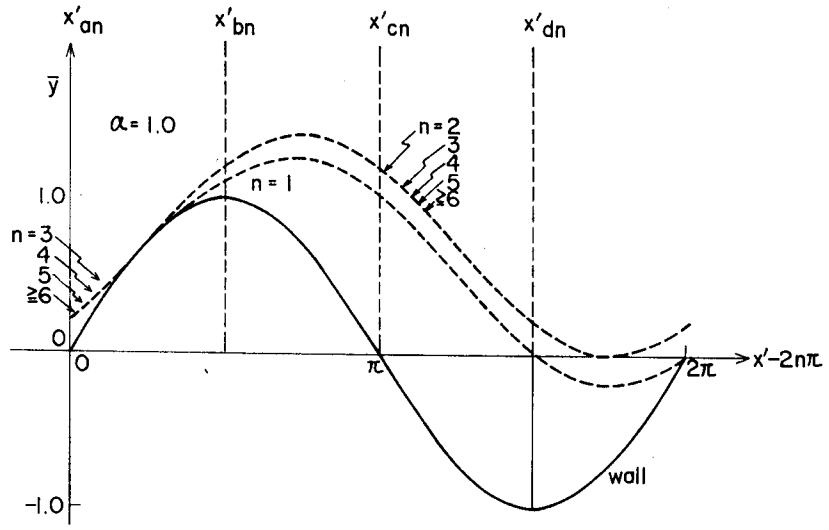

Fig. 9. Limiting particle streamline for $\alpha=1.0$.

$$x'_{an}=2n\pi\,,\quad x'_{bn}=\left(2n+\frac{1}{2}\right)\pi\,,\quad x'_{cn}=(2n+1)\pi\,,\quad x'_{dn}=2\left(n+\frac{3}{2}\right)\pi\,,$$

where $n=0$ to 6, which are indicated in Figure 9. As shown in Figures 10 to 16, the flow structure at each point x' is not simple. In all cases, the velocity distribution has a minimum at some point of $\bar{\eta}$. The absolute value of $\partial u/\partial\bar{\eta}$ increases with $x'(n)$, especially in the region very close to the wavy wall. Theoretically, it is expected that $\partial u/\partial\bar{\eta}$ at $\bar{\eta}=0$ will tend to a negative infinity as $x'\to\infty$, since the particle impingement on the wavy wall substantially ceases as $x'\to\infty$. Then, the limiting particle streamline becomes tangential with the wall boundary only at one point in the unit interval (unit wavelength) as $x'\to\infty$. This situation is shown in Figure 9. The effect of the existence of particle-free regions on the distribution of u can easily be seen from Figures 10 to 16.

It may be said that the velocity change with $\bar{\eta}$ is relatively more distinguished in the dust-free region than in the dusty region.

In Figure 17, the distributions of u at $x'=2n\pi$ ($n=0$ to 6) are shown, which correspond to the results in Figures 10 to 16. This demonstrates the detailed change of the velocity distribution u along $\bar{\eta}$ with x' (or n). It is important to realize that the velocity distributions appreciably change with x' or n. Such a situation is very different from that for the outer solution. Mathematically, it will be sure that the flow structure in the inner region as well as the outer region becomes completely periodic as $x'\to\infty$. Then, the velocity distribution u at

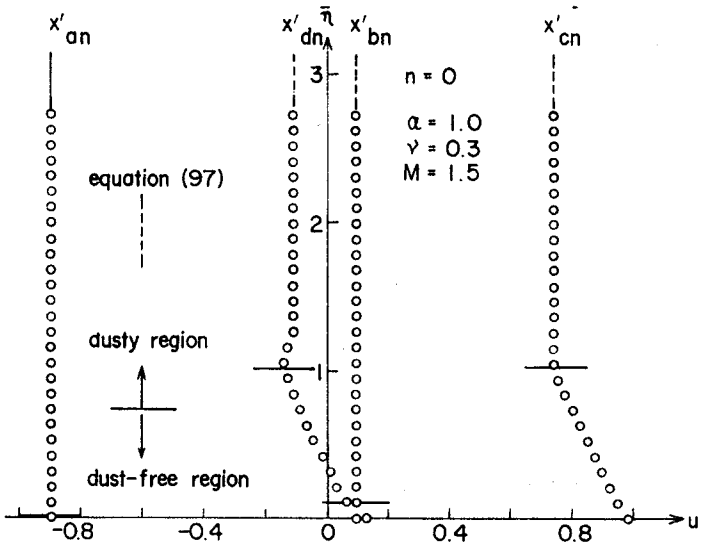

Fig. 10. Distribution of u along $\bar{\eta}$ in the inner layer.

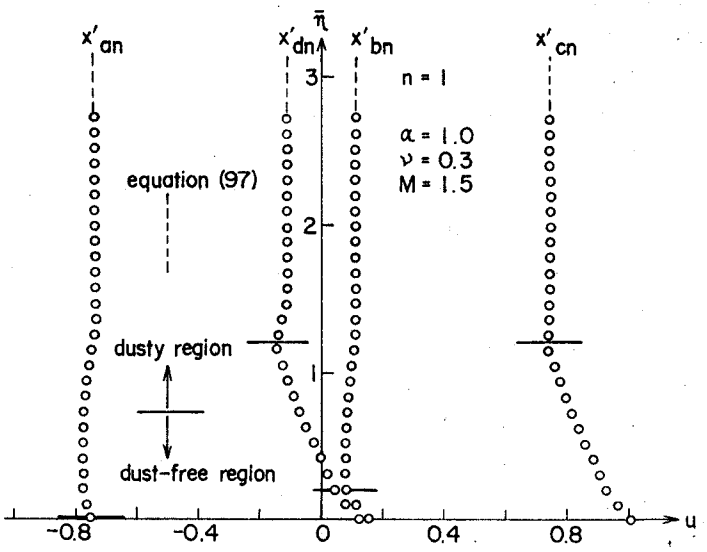

Fig. 11. Distribution of u along $\bar{\eta}$ in the inner layer.

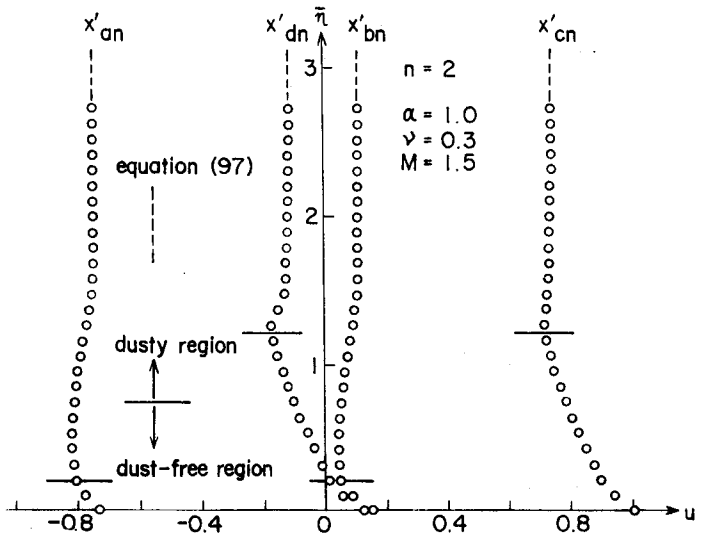

Fig. 12. Distribution of u along $\bar{\eta}$ in the inner layer

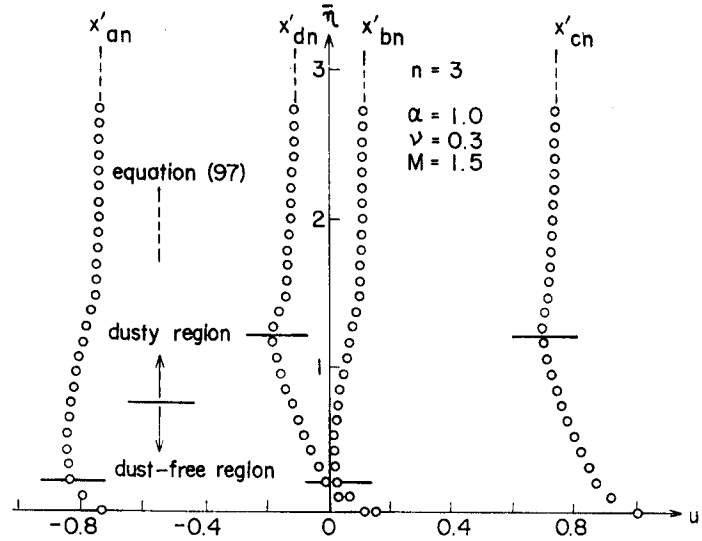

Fig. 13. Distribution of u along $\bar{\eta}$ in the inner layer.

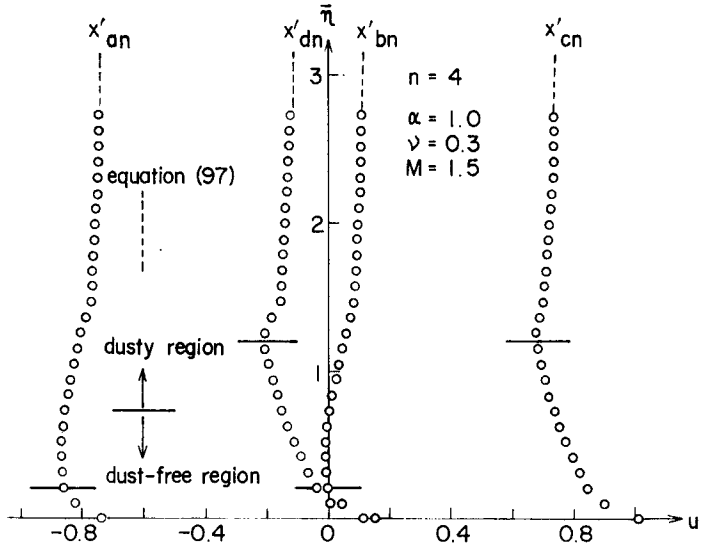

Fig. 14. Distribution of u along $\bar{\eta}$ in the inner layer.

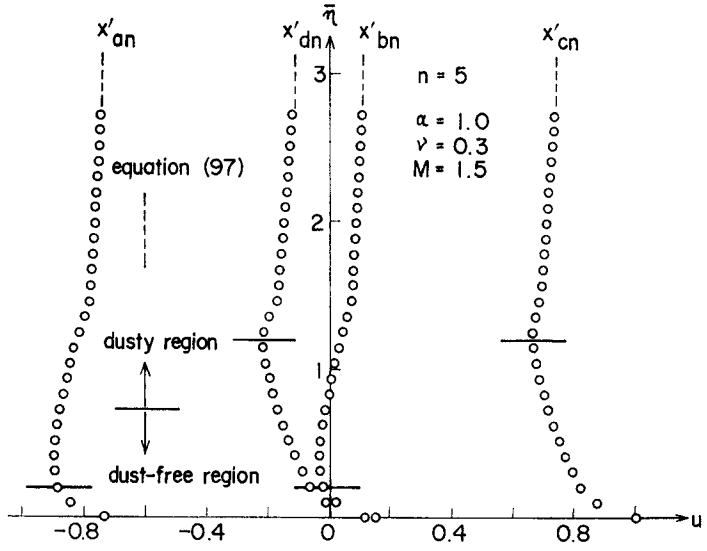

Fig. 15. Distribution of u along $\bar{\eta}$ in the inner layer.

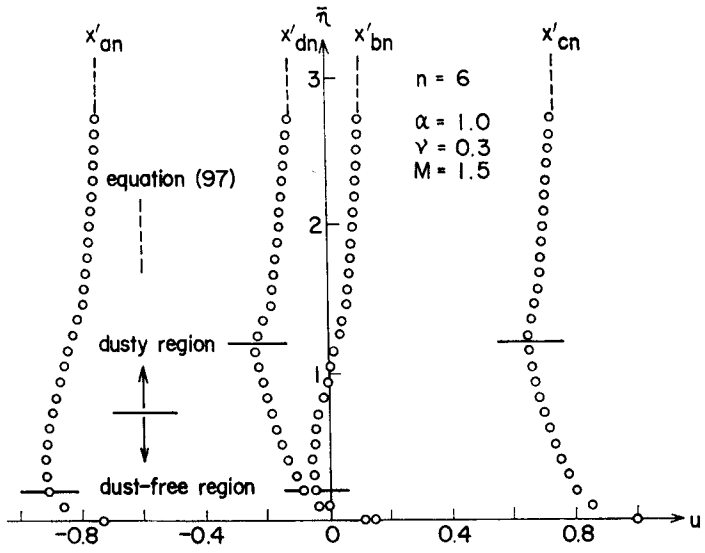

Fig. 16. Distribution of u along $\bar{\eta}$ in the inner layer.

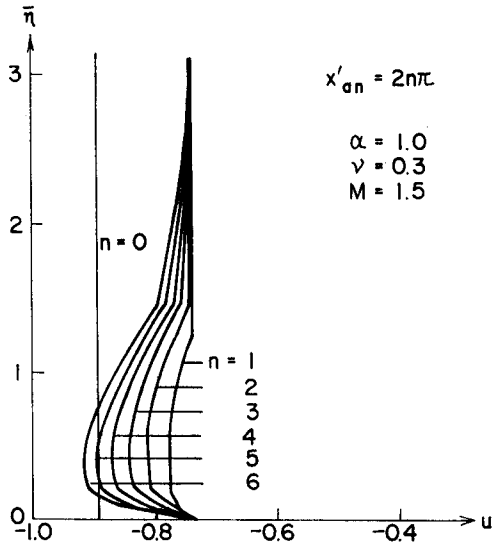

Fig. 17. Distribution of u along $\bar{\eta}$ in the inner layer at $x'=x'_{an}$.

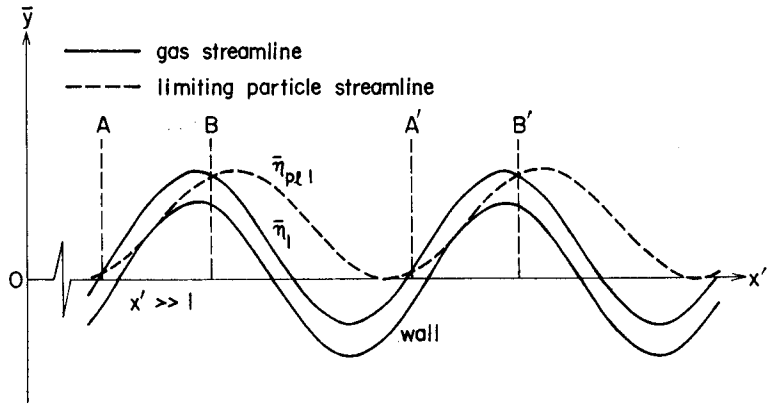

Fig. 18. Gas streamline near the wavy wall.

x'_{an} (also at x'_{bn}, x'_{cn} and x'_{dn}) will converge to some fixed distribution. Figure 17, however, does not show such a trend clearly, which suggests the fact that it takes a very large distance along x' from the origin for the inner flow to become sufficiently periodic.

In order to explain this situation, Figure 18 will be quite helpful, where the gas and the limiting particle streamlines for a large x' are schematically shown. Referring to Figure 18, let us denote a gas streamline near the wavy wall by $\bar{\eta}=\bar{\eta}_1$ (solid line) and a limiting particle streamline by $\bar{\eta}_{pl}=\bar{\eta}_{pl1}$ (dotted line). The gas element along $\bar{\eta}=\bar{\eta}_1$ flows through the dusty region only between points A and B (or A′ and B′) per unit wavelength. Since the adjustment of the flow quantities of the gas along the streamline $\bar{\eta}=\bar{\eta}_1$ with those of the particles is possible only while the gas remains in the dusty regions AB and A′B′ ⋯, the length along x', necessary for the flow quantities of the gas along $\bar{\eta}=\bar{\eta}_1$ to be adjusted completely with those of the particles, will naturally be very large. This is greatly enhanced for the gas along a streamline very close to the wavy wall. However, the difference between the flow quantities of the gas at the points x' and $x'+2\pi$ along the streamline very close to the wavy wall becomes very small in magnitude, especially for a large x'. This is because the total amount of particles, with which the gas can interact per unit interval, is very small. The results for $\bar{\eta}\ll 1$ and $n>3$ in Figure 17 well demonstrate this situation.

Although it will be very important and interesting to obtain the converged velocity distribution u along $\bar{\eta}$ as $n\to\infty$ or the limiting periodic structure of the inner solution as $x'\to\infty$, unfortunately it could not be done here because of a numerical difficulty. As has been discussed previously, a very large distance along x' from the origin is necessary to obtain the final periodic inner solution,

which inevitably leads to the necessity of a great number of mesh numbers for reliable numerical calculations. In the present paper, only the results, for which the numerical accuracy could be checked, are shown.

Finally, the velocity u and the pressure p of the gas in the outer region for $x' \gg 1$ have been calculated from Equations (110) and (115) in conjunction with (111) and (114). As will be seen from their derivation, the flow quantities are completely periodic with respect to x'. Mathematically, these results are valid with order ε for $O(x') > \frac{1}{\alpha}|\log \varepsilon|$. Since Equation (115) yields $\psi(x')$ in Equation (49) as $y' \to 0$, the gas pressure on the wavy wall is obtained as

$$p = \psi(x') = -\frac{\gamma M^2}{\sqrt{A^2+A^2}}\left\{\sin(x'-\delta) - \frac{\nu\alpha}{\sqrt{\alpha^2+1}}\cos(x'-\delta+\delta_p)\right\}. \quad (116)$$

Similarly, from Equations (110) and (112), we can get

$$u = \frac{1}{\sqrt{A^2+A^2}}\sin(x'-\delta), \quad (117)$$

$$u_p = -\frac{\alpha}{\sqrt{\alpha^2+1}}\frac{1}{\sqrt{A^2+A^2}}\cos(x'-\delta+\delta_p). \quad (118)$$

The numerical results for Equations (116) to (118) have shown an almost complete agreement with those for Equations (97), (98), and (101) obtained by means of the Laplace transform for $x' \gg 1$. These are, therefore, not shown here.

It will be possible to prove mathematically that the solutions (97), (98), and (101) agree, respectively, with (112), (113) and (111) in the limit of $x' \to \infty$. Here, however, we do not discuss this proof, because an excellent agreement between the corresponding numerical results has been obtained. Also, the mathematical procedures applied to obtain these two sets of solutions automatically warrant the agreement of the corresponding results in the limit $x' \to \infty$.

Drag Coefficient

Consider the drag coefficient of the wavy wall. To the accuracy required in the two-dimensional small disturbance case, the pressure coefficient $C_p = (P-P_0)/\frac{1}{2}\rho_0 U_0^2$ can be found to be

$$C_p = \frac{2\varepsilon}{\gamma M^2}p. \quad (119)$$

If we denote the drag coefficient per unit wavelength in the range $(n-1)l \leqq x \leqq nl$ $(2(n-1)\pi \leqq x' \leqq 2n\pi)$ $(n=1, 2, 3, \cdots)$ by C_{dn}, it can be calculated from

$$C_{dn}=\frac{1}{2\pi}\int_{x'_{an-1}}^{x'_{an}}(C_p)_w\frac{dy'_w}{dx'}dx', \tag{120}$$

where $(C_p)_w$ is the value of C_p evaluated at the wall. Substituting Equation (119) into (120) yields

$$C_{dn}=\frac{\varepsilon^2}{\pi\gamma M^2}\int_{x'_{an-1}}^{x'_{an}}\psi(x')\cos x'dx'. \tag{121}$$

Especially for $x'\gg 1$, Equation (116) can be used as $\psi(x')$ in Equation (121), and the explicit result is obtained as

$$C_{dn}=\frac{\varepsilon^2}{\Delta^2+\Lambda^2}\left\{\Lambda+\frac{\nu\alpha}{\alpha^2+1}(\Delta+\Lambda\alpha)\right\}. \tag{122}$$

Since the flow structure is completely periodic in the limit of x' (or n)$\to\infty$, this result does not depend on the number n. For the small number n, however, C_{dn} given by (121) depends on n. With Equation (101), Equation (121) was calculated, and the result is shown in Table 2. For $n\geqq 2$, C_{dn} is almost constant and is equal to the result of Equation (122).

It must be emphasized that the drag coefficient (121) represents only the contribution of the gas pressure. If the effect of the particle impingement on the wall on the drag coefficient is taken into account, it is necessary to evaluate the contribution of the particle impingement to this coefficient. Denoting it by C_{dpn},

$$C_{dpn}=\frac{1}{2\pi}\int_{x'_{pni}}^{x'_{pnf}}\left(\frac{\rho_{pw}V_{pxw}^2}{\frac{1}{2}\rho_0U_0^2}\right)\frac{dy'_w}{dx'}dx', \tag{123}$$

where $V_{fx}=U_0(1+\varepsilon u)$ and x'_{pni} and x'_{pnf} are the initial and the final points of the particle impingement region on the wall in the range $2(n-1)\pi\leqq x'\leqq 2n\pi$.

Table 2. Drag coefficient of the wavy wall for $a=1.0$, $\nu=0.3$, and $M=1.5$.

n	C_{dn}/ε^2	C_{dpn}/ε
1	0.8727	0.04847
2	0.8694	0.01902
3	0.8694	0.00004
4	0.8694	0.00000
$\geqq 5$	0.8694	0.00000
	calculated with Eq. (101)	Eq. (124)
∞	0.8694	0
	Eq. (122)	

When there exist two distinct particle impingement regions in a unit interval, which is possible for a large α, the contributions from these two regions must be summed up. Also, when the point $x'=2n\pi$ is located in a particle impingement region, x'_{pni} or x'_{pnf} in Equation (123) must be replaced by $x'=2n\pi$.

In terms of the perturbation quantities, C_{dpn} can be rewritten in the form

$$C_{dpn} = \varepsilon \frac{\nu}{\pi} (\sin x'_{pnf} - \sin x'_{pni}) + O(\varepsilon^2) , \tag{124}$$

which indicates that the contribution to the drag coefficient of the particle impingement on the wall is order ε, and is larger than the gas phase contribution by one order. The numerical results are shown in Table 2. This shows that the contribution C_{dpn} is important only for a small number n or only for the front part of the wavy wall.

Conclusions

The first-order perturbation problem of a gas-particle two-phase flow over a wavy wall has been analyzed. It was proved that the location of particle-free regions is determined only by two parameters, the particle parameter α and the wall parameter ε. It does not depend on the loading ratio ν. It is interesting to note that there exist regions of a high velocity gradient adjacent to the wall surface. Of course, all the present results have been obtained under the condition that the gas is inviscid, except for its interaction with the particles. If the gas phase is not assumed to be inviscid, the boundary layer in the region adjacent to the wall and its interaction with the present inner flow must be taken into account in the analysis of the inner problem. In such a case, however, the problem will become desperately complicated and difficult.

The drag coefficient of the wavy wall was obtained. In the case of two-phase flows, the particle contribution to the drag coefficient due to the particle impingement on the wall will be very important, because its contribution is larger than the gas phase contribution by one order.

APPENDIX A

If we consider the second-order inner expansion as

$$\boldsymbol{V}_p = U_0(\boldsymbol{i} + \varepsilon \boldsymbol{q}_{p1} + \varepsilon^2 \boldsymbol{q}_{p2} + O(\varepsilon^3)) ,$$
$$\rho_p = \rho_{p0}(1 + \varepsilon \sigma_{p1} + \varepsilon^2 \sigma_{p2} + O(\varepsilon^3)) ,$$
etc.,

Equation (5) yields

$$\frac{\partial v_{p1}}{\partial \bar{y}} = 0,$$

$$\frac{\partial \sigma_{p1}}{\partial x'} + \frac{\partial u_{p1}}{\partial x'} + v_{p1} \frac{\partial}{\partial \bar{y}} (\sigma_{p1} + v_{p2}) = 0.$$

This suggests that the second-order expansion is necessary to determine σ_{p1} in the present analysis.

APPENDIX B

The wave from the origin propagates along the line

$$\frac{dy'}{dx'} = 1/\sqrt{M^2-1} \quad \text{or} \quad y' = x'/\sqrt{M^2-1} \qquad (M>1),$$

which can be represented in the $x'\bar{y}$ coordinate system as

$$\bar{y} = \frac{1}{\sqrt{M^2-1}} \frac{x'}{\epsilon}.$$

This means that the wave propagates along

$$x' = 0 \tag{B-1}$$

in the present first-order inner problem. Since the usual classical relations hold for the dust-free gas just behind the wave (B-1), we have Equations (76) and (77). The particle quantities are continuous across the wave (B-1), leading to the results (78) and (79).

APPENDIX C

The solutions for Equation (92) are given by

$$\begin{bmatrix} -\lambda_1 \\ -\lambda_2 \end{bmatrix} = \frac{-\Gamma_1(a+b) \pm \sqrt{D}}{2\Gamma_0}$$

where

$$D = (a+b)^2\Gamma_1^2 - 4ab\Gamma_0\Gamma_2.$$

With Equation (86), this can be rewritten as

$$D = \left\{ M^2 \left[a(1+\nu) - b\frac{(1+\gamma\nu\theta)}{(1+\nu\theta)} \right] - (a-b) \right\}^2 + 4M^2ab\frac{(\gamma-1)\nu^2\theta}{(1+\nu\theta)}.$$

Since $\gamma>1$, this shows $D>0$, which indicates λ_1 and λ_2 are real. Moreover, it is easy to see that both λ_1 and λ_2 are positive for $\Gamma_0>0$ $(M>1)$.

APPENDIX D

The formula for the inverse Laplace transform used in deriving Equations (97) and (98) are as follows:

$$L^{-1}[\hat{f}_i(s+k)] = \exp(-kx')f_i(x') ,$$

$$L^{-1}[\hat{f}_i(s)\hat{f}_j(s)] = \int_0^{x'} f_i(z)f_j(x'-z)dz ,$$

$$L^{-1}\left[\left(\frac{s+k}{s-k}\right)^{1/2}\right] = k\{I_0(kx')+I_1(kx')\}+\delta(x') ,$$

$$L^{-1}\left[\frac{1}{s}\left(\frac{s+k-r}{s+k+r}\right)^{1/2}\right] = \exp(-kx')I_0(rx')+(k-r)\int_0^x \exp(-kz)I_0(rz)dz ,$$

$$L^{-1}[(s^2+ks+r)^{-1/2}] = \exp\left(-\frac{1}{2}kx'\right)I_0\left(\sqrt{\frac{1}{4}k^2-r}x'\right) ,$$

where L^{-1} denotes the inverse Laplace transform, $\delta(x')$ is the Dirac delta function, z is a dummy variable, and k and r are constants.

References

Carrier G.F. 1958 J. Fluid Mech. 4, 376.

Clarke J.F. 1959 J. Fluid Mech. 7, 37.

Erdelyi A., Magnus W., Oberhettiger F. & Tricomi F.G. 1954 Tables of Integral Transforms, vol. 1. New York, MacGlaw-Hill.

Ishii R. & Kawasaki K. 1982 The Physics of Fluids 25, 959.

Ishii R. & Matsuhisa H. to be published in J. Fluid Mech..

Marble F.E. 1963 AIAA J. 12, 2793.

Miura H. 1974 J. Phys. Soc. Japan 37, 1145.

Rudinger G. 1970 Nonequilibrium Flows 1. Marcel Dekker, 119.

Takano A. & Adachi T. 1975 Trans. J. Soc. Aero. Space Sci. 42, 197.

Vincenti W.G. 1959 J. Fluid Mech. 6, 481.

Zucrow M.J. & Hoffman J.D. 1977 Gas Dynamics 2, John Wiley and Sons, 278.